

Synthetic Methods

A Functional Hexaphenylbenzene Library Comprising of One, Three, and Six Peripheral Rylene-Diimide Substituents

Carolin Dusold,^[a] Benedikt Platzer,^[b] Philipp Haines,^[b] David Reger,^[a] Norbert Jux,^[a] Dirk M. Guldi,^[b] and Andreas Hirsch^{*[a]}

Abstract: Synthesis and characterization of a series of rylene-diimide substituted hexaphenylbenzenes (HPBs) is presented. The direct connection of the rylene-diimide units to the HPBs via the imide-N-position without any linkers as well as the use of naphthalene-diimides (NDIs) next to perylene-diimides (PDIs) is unprecedented. While mono-substituted products were obtained by imidization reactions with amino-HPB and the respective rylene-monoimides, key step for the formation of tri- and hexa-substituted HPBs is the Co-catalysed cyclotrimerization. Particular emphasis for

physic-chemical characterization was on to the number of NDIs/PDIs per HPB and the overall substitution patterns. Lastly, Scholl oxidation conditions were applied to all HPB systems to generate the corresponding hexa-*peri*-hexabenzocoronenes (HBCs). Importantly, the efficiency of the transformation strongly depends on the number of NDIs/PDIs. While three rylene-diimide units already hinder the Scholl reaction, the successful synthesis of mono-substituted HBCs is possible.


Introduction


Rylene-diimides, in general, and perylene-diimides (PDIs), in particular, have been successfully used as suitable electron acceptors in organic electronics such as organic solar cells (OSCs) and organic field effect transistors (OFETs).^[1] They offer excellent electron mobility, high thermal, chemical, and photochemical stabilities and a suitable absorption range, which makes them so far the most common non-fullerene small molecular acceptors (SMAs).^[2] However, a great drawback is the tendency of rylene-diimides to form large domains due to intermolecular aggregation stemming from their planar cores.^[3] Thus, gaining control over size and supramolecular organisation is crucial in terms of SMA-applications and SMA-performances in organic electronics.^[4] To overcome this strong aggregation, molecular architectures featuring multiple rylene-diimides and different

structural features have already been synthesized for efficient solar-energy harvesting.^[5] In polymeric and star-shaped rylene-diimide derivatives aggregation is suppressed and, in turn, improved efficiencies and better photovoltaic performances were noted. In this context, a particularly promising candidate turned out to be hexaphenylbenzene (HPB). Its hexagonal symmetry is suitable for constructing star-like architectures. For example, propeller-shaped molecular acceptors with six peripheral PDIs attached to a HPB core via their bay-position have been synthesized and investigated with respect to their photo-physical properties.^[6] It was found that in the resulting 3D geometry the planarity of the structure is reduced and aggregation is prevented leading to excellent OSC efficiencies. Another interesting aspect regarding HPBs as a linker is the possibility to convert them into the corresponding planar hexa-*peri*-hexabenzocoronenes (HBCs) via oxidative cyclodehydrogenation (Scholl reaction).^[7] HPB-to-HBC transformation renders excellent electron donors with interesting electronic properties, very high charge carrier mobility, and unique self-assembly behaviour.^[8] Such D-A dyads consisting of HBCs as electron donors (D) and rylene-diimides as electron acceptors (A) have recently attracted wide-spread attention as materials in optoelectronic devices.^[9,4] One major benefit of these HBC-rylene-diimide conjugates is the possibility to navigate self-organization. They generate well-ordered supramolecular structures which offer full control of the orientation of the units to each other. In this work, we report on a library of rylene-diimide-HPB conjugates, varying the number of rylene units attached to the HPB core (Figure 1). The major synthetic strategy via (mixed-)cyclotrimerization reactions was carried out in a manner similar to that used for the analogous porphyrin-HPB systems.^[10] The reaction products are categorized into mono-, tri-, and hexa-substituted

[a] C. Dusold, D. Reger, Prof. Dr. N. Jux, Prof. Dr. A. Hirsch
Department of Chemistry and Pharmacy
Friedrich-Alexander-University Erlangen-Nuremberg
Nikolaus-Fiebiger-Straße 10, 91058 Erlangen (Germany)
E-mail: andreas.hirsch@fau.de

[b] B. Platzer, P. Haines, Prof. Dr. D. M. Guldi
Department of Chemistry and Pharmacy
Friedrich-Alexander-University Erlangen-Nuremberg
Egerlandstraße 3, 91058 Erlangen (Germany)

 Supporting information and the ORCID identification number(s) for the author(s) of this article can be found under <https://doi.org/10.1002/chem.202004273>.

 © 2020 The Authors. Chemistry - A European Journal published by Wiley-VCH GmbH. This is an open access article under the terms of the Creative Commons Attribution Non-Commercial NoDerivs License, which permits use and distribution in any medium, provided the original work is properly cited, the use is non-commercial and no modifications or adaptations are made.

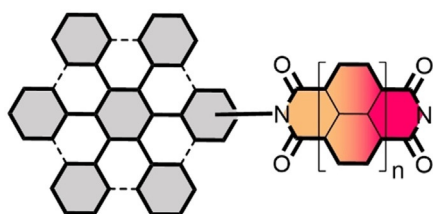


Figure 1. Rylene-diimide HPB conjugates.

conjugates, with a C₃-symmetric and a less symmetric isomer in case of the tri-substituted compounds.

In contrast to previous reports,^[6] in which the PDIs are connected to the HPB/HBC via either ethynyl-units or the PDI bay-position, we opted for no linkers between the rylene-diimides and the HPBs to maximize intramolecular communications and rigidify the molecular structure. Additionally, the rylene-diimides are connected via the imide-*N*-position to further investigate this binding motif in such systems. Furthermore, we extended the concept of PDI-HPBs ($n=2$) to naphthalene-diimides (NDI, $n=1$) to compare them in relation to their efficiency as SMAs. So far, PDI-HBCs were exclusively synthesized via cross-coupling reactions of pre-formed HBCs and PDIs.^[9a,4] In this contribution, we expand the synthetic access of such conjugates by examining the Scholl-type oxidation of the corresponding HPBs to generate covalently linked HBC-rylene-diimide D-A dyads. Finally, the physicochemical properties of all new conjugates were investigated.

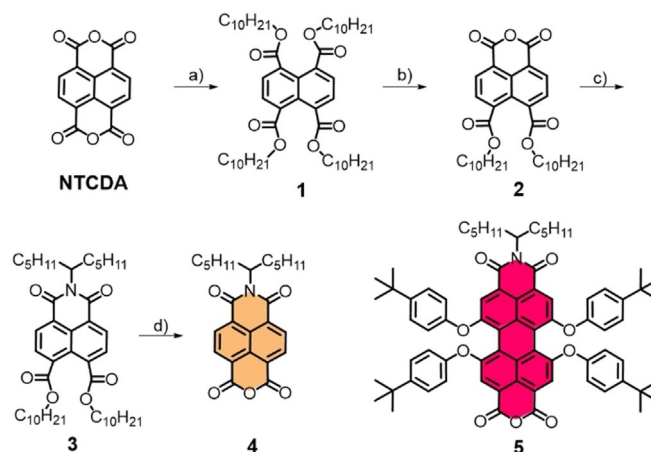
Results and Discussion

Synthesis and characterization

Rylene-monoimides **4** and **5** were chosen as starting material for the synthesis of rylene-diimide-HPBs. Naphthalene-monoimide **4** was synthesized via the “ester-route”^[11] as depicted in Scheme 1. It enables the generation of the monoimide in a directional, large scale synthesis (gram amounts) compared to previously reported synthetic sequences,^[9e,12] which are not applicable in our case, using the 6-undecyl-swallow tail. The first step of the synthetic route was the formation of tetraester **1**, which was transformed to the monoimide diester **2** by means of acidic hydrolysis. By mixing **2** with undecyl-amine in imidazole followed by a second hydrolysis to remove the two remaining dodecyl-ester groups naphthalene-monoimide **4** was synthesized in an overall yield of 15% (see the Supporting Information for synthetic details).

For the synthesis of perylene-monoimide **5** a modified literature procedure was used^[13] (see the Supporting Information for synthetic details). In particular, perylene-dianhydride was bay-functionalized with four *tert*-butyl-phenoxy substituents to prevent aggregation and/or π -stacking. The bulky substituents force a twisting out of the perylene plane and, therefore, increase solubility, which is important for the synthesis, purification, and characterization.^[14]

We started with the synthesis of mono-substituted NDI- as well as PDI-HPB conjugates following the synthetic procedure

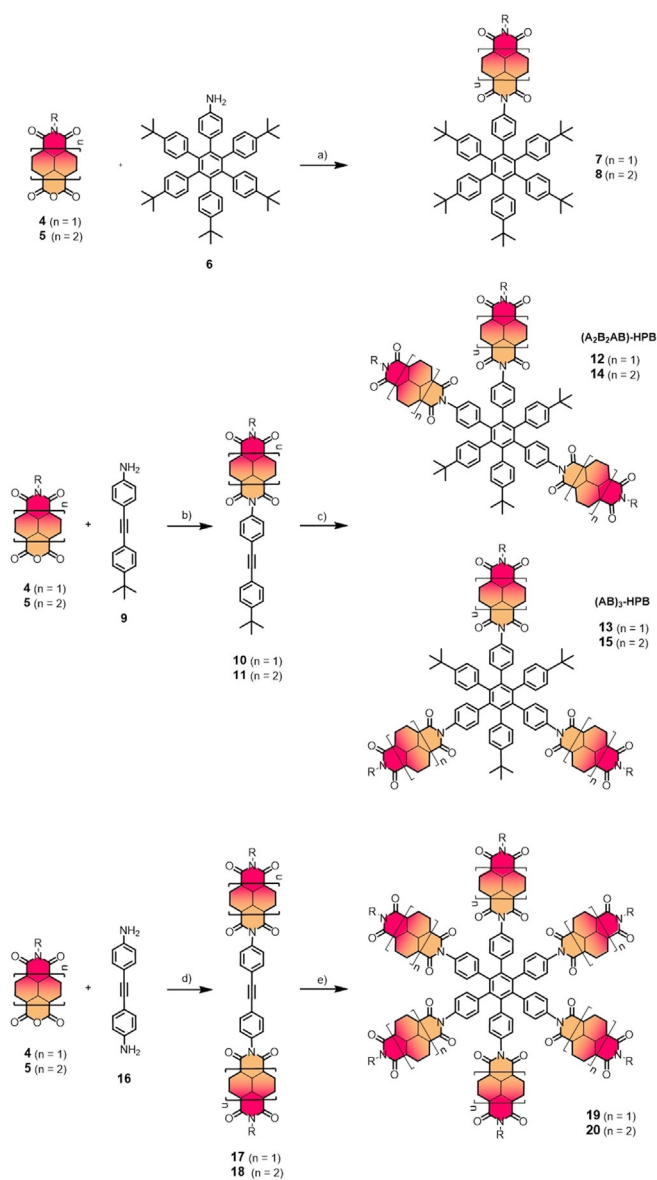


Scheme 1. Synthesis of naphthalene-monoimide **4** (orange); bay-substituted perylenemonoimide **5** (pink). a) DBU, decylbromide, decanol, DMF, rt, 48 h, yield 74% b) pTsOH, toluene:dodecane 1:5, 95 °C, o.n., yield 60% c) amine, imidazole, 150 °C, 1 h, yield 78% d) pTsOH, toluene:dodecane 1:5, 95 °C, o.n., yield 44%.

depicted in Scheme 2. Amino-HPB **6** was synthesized as previously reported.^[15] Imidization-reaction of the rylene-monoimides with amino-HPB **6** results in the formation of the corresponding NDI-HPB **7** and PDI-HPB **8** in 72% and 31% yields, respectively. For the formation of the tri-substituted as well as the hexa-substituted conjugates we used a different synthetic approach, that is, the Co-catalysed cyclotrimerization reaction. It allows to control the substitution pattern on the HPB. Therefore, mono- and di-substituted rylene-diimide-tolane precursors are essential. To generate the mono-rylene-diimide precursors **10** and **11**, standard palladium-catalysed Sonogashira cross-coupling reactions of ethynyl-benzene with 4-iodo-*tert*-butyl-benzene were utilized (Supporting Information) to afford amino-tolane **9**^[16] to which rylene-monoimides **4** and **5** were coupled *via* an imidization reaction.

NDI-tolane **10** as well as PDI-tolane **11** was then reacted under cobalt carbonyl catalysis in refluxing toluene. After heating for 18 h, complete conversion of the starting material was observed. During the reaction two isomers are formed, an C₃-symmetric (AB)₃-HPB and a less symmetric (A₂B₂AB)-HPB (Scheme 2). The two NDI-HPB isomers **12** and **13** were successfully separated by column chromatography. The yield of the less symmetric NDI₃-HPB-u **12** was 53%, while that of the C₃ symmetric NDI₃-HPB-s **13** was 17%, which corresponds to a 3:1 ratio of 1,2,4- and 1,3,5-substitution pattern. This is in accordance with the expected selectivity, which has been reported for similar cyclotrimerization reactions.^[17] Similar results were observed for the cyclotrimerization reaction of the PDI-derivative **11**. In this particular case we were able to separate the less symmetric (**14**) and the C₃-symmetric (**15**) isomers by column chromatography in a pure form in 66% and 17% yields, respectively. Assignment of the two isomers was done by ¹H-NMR-spectroscopy. The aromatic region of NDI-HPBs are depicted in Figure 2 (left).

In the case of NDI₃-HPB-u **12**, the 24 protons of the benzene-rings of the HPB-unit appear as several complex overlap-



Scheme 2. Synthesis of rylene-diimide-HPBs. a) Imidazole, 140 °C, 2–4 h, yield 72 % (7) and 31 % (8) b) imidazole, 120 °C, 0.5–1 h, yield 49 % (10) and 50 % (11) c) $\text{Co}_2(\text{CO})_8$, toluene, 140 °C, 18 h, yield 53 % (12), 17 % (13), 66 % (14) and 17 % (15) d) imidazole, 120 °C, 1 h, yield 42 % (17) and 27 % (18) e) $\text{Co}_2(\text{CO})_8$, toluene, 140 °C, 18 h, yield 61 % (19) and 56 % (20).

ping multiplets between 6.78–7.09 ppm. Due to a higher symmetry, these protons within the C₃-symmetric NDI₃-HPB-s **13** emerge only as four partially overlapping pseudo-doublets, each with an integral ratio of six. A similar trend was observed for PDI derivatives **14** and **15** (Figure 2, right), with additional signals for the *tert*-butyl-phenoxy bay-substituents at around 6.85 and 7.25 ppm. Next, we examined the Co-catalysed cyclotrimerization of bis-rylene-diimide-tolanes. For the synthesis of diamino-tolane **16** literature synthetic procedure was used.^[18] Addition of the rylene-monoimides results in the formation of the di-substituted tolans **17** and **18**, followed by cyclotrimerization (Scheme 2). The reactions were performed under similar conditions as the previous ones, however, to obtain good conversion, a larger amount of cobalt catalyst (0.75 equiv) is required. Thus, NDI₆-HPB **19** as well as PDI₆-HPB **20** were successfully synthesized in good yields of 61 % and 56 %, respectively. Since the hexa-substituted derivatives exhibit C₆-symmetry, the 24 HPB protons appear only as two pseudo-doublets at 7.08 and 7.02 ppm for NDI₆-HPB **19**. In case of the PDI-derivative **20**, the HPB signals are located at around 6.84 and 6.98 ppm, with additional resonances of the bay-substituent in the region of 6.73–7.23 ppm (Figure 2, bottom). Comparing the ¹H-NMR spectra of mono-, tri-, and hexa-substituted NDIs as well as PDIs with references **4** and **5**, suggests a relationship between substituents and aggregation. An increased substitution degree results in a high-field shift of the NDI- as well as PDI-core protons (see Figures S45 and 46). This is attributed to closer π -interactions of the ryleneimides in solution. For more detailed information regarding the nature of the association further investigations are needed.

As the final reaction step, Scholl-oxidation reaction was used to generate the corresponding HBC-derivatives. Three reaction conditions using different acids and oxidizing reagents, namely FeCl_3 , DDO^[19] and PIFA/ $\text{BF}_3 \cdot \text{Et}_2\text{O}$,^[19b,20] were investigated (see Table S1). Unfortunately, the tri-substituted and the hexa-substituted rylene-diimide-HPBs did not close to the planar HBC structure, no matter which reaction condition was used. Instead, the starting material was recovered. One reason could be the pronounced electron deficiency of the corresponding HPB cores, caused by the increased number of electron withdrawing/accepting rylene-diimide substituents. As a result, oxi-

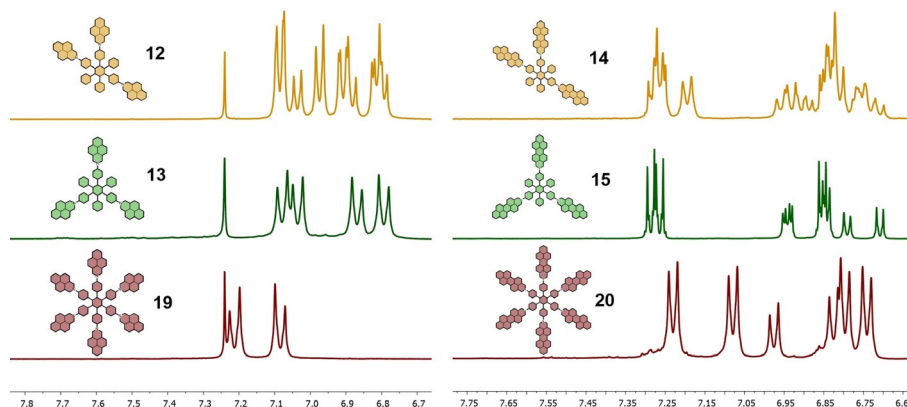
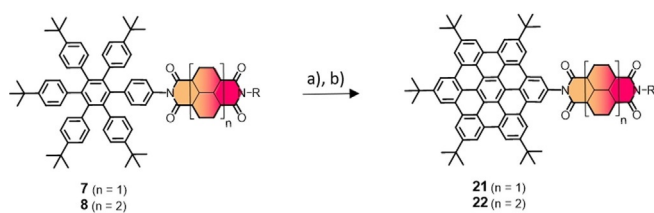


Figure 2. Aromatic region of ¹H NMR spectra of tri-substituted and hexa-substituted rylene-diimide-HPBs; left: NDI-HPBs **12**, **13**, **19**; right: PDI-HPBs **14**, **15**, **20**.



Scheme 3. Synthesis of mono-substituted rylene-diimide-HBCs **21** and **22**. a) **7**, FeCl_3 , CH_3NO_2 , DCM, 0°C , o.n., yield 85% b) **8**, FeCl_3 , CH_3NO_2 , DCM, -78°C , o.n., yield 61%.

dative cyclodehydrogenation is prevented, which is in accordance with observations found for multiple-porphyrin functionalized HBCs.^[21] However, we were successful to synthesize mono-substituted rylene-diimide-HBCs (Scheme 3).

Initially the reaction was performed in DCM at 0°C using FeCl_3 as oxidizing agent (reaction condition a)). Thereby, NDI-HBC **21** was generated in a good yield of 85%. The $^1\text{H-NMR}$ spectra of the NDI-derivatives (Figure 3, left) confirm the successful transformation of HPB **7** to HBC **21**. After planarization, the resonance of the HPB between 6.68–7.01 ppm disappeared completely. At the same time, new downfield shifted signals at 9.10–9.30 ppm emerge, which can be assigned to the 12 aromatic protons of the HBC-moiety.

Applying the same reaction conditions to the conversion of PDI-HPB **8**, we failed to isolate any product. Instead, noticeable amounts of decomposition-products were detected by TLC. Performing, however, the reaction at a lower temperature of -78°C (reaction condition b)) results in the successful formation of the product in good yield of 61%. $^1\text{H-NMR}$ spectroscopy confirmed the formation of HBC **22** (Figure 3, right). Again, new downfield shifted resonances for the coronene unit between 9.15–9.41 ppm are found, while simultaneously the HPB signals disappear.

UV-vis absorption and fluorescence emission studies

Absorption and fluorescence were investigated for all compounds. The UV-vis absorption spectra of NDI-HPBs **7**, **12**, **13**, and **19** (Figure 4A) show the characteristic absorption of NDI at 360 and 380 nm with a shoulder at 343 nm. The absorption spectra of PDI-HPBs **8**, **14**, **15**, and **20** are shown in Figure 4B and exhibit major absorption maxima at 450, 538, and 577 nm.

For both NDI- as well as PDI-containing compounds an increased molar extinction coefficient is observed with respect to the number of rylene-diimide-units.

The transformation of the mono-rylene-diimide HPBs to the corresponding HBCs are monitored by UV-vis absorption spectroscopy as well. After Scholl oxidation, NDI-HBC **21** displays a new strong HBC-based absorption signature at 360 nm (Figure 4C), thereby overlapping with the NDI-absorptions. PDI-HBC **22** exhibits a similar coronene-centred absorption at around 360 nm once the system is closed (Figure 4D). At the same time, the PDI absorption decreases slightly in intensity and experiences a red-shift of 5 nm to 582 nm, which prompts to electronic communications between PDI and HBC.

Fluorescence assays with NDIs and PDIs were performed in both toluene and PhCN. Adequate spectra of the NDIs were, however, only discernible at higher concentrations in DCM (Figure 5A) due to their moderate fluorescence quantum yields. NDI-HPBs show fluorescence maxima at 395 nm for **7** and at 402 nm for **12**, **13**, and **19**. Stokes shifts of 15–22 nm result accordingly, when compared with their 380 nm absorptions (Figure S51). The NDI-fluorescence strongly broadens when going from the mono-substituted **7** to the tri-substituted **12** and **13** and finally to the hexa-substituted **19**. The fluorescence spectrum of NDI-HBC **21** mostly consists of the characteristic HBC features at 470 and 500 nm. All NDIs with the exception of NDI-HPB **7** also show a weaker feature at 534 nm, likely a result of NDI-NDI interaction.

This interaction is probably enabled by the short distance between NDIs in the trimers and the hexamer, while π - π -stacking of the HBC in **21** may also result in multiple NDIs in close vicinity to each other. Fluorescence spectra of the PDI-HPBs feature bands at 595 nm (**8**) and 598 nm (**14**, **15**, **20**) with shifts around 20–25 nm in toluene (Figure 5B). The fluorescence of PDI-HBC **22** appears red-shifted at 603 nm. Much larger Stokes shifts of around 30 nm occur in PhCN with strongly shifted fluorescence maxima at 611, 612, and 615 nm for the PDI-HPB monomer, trimers, and hexamer, respectively (Figure S52). The fluorescence of the PDI-HBC **22** is heavily quenched at 611 nm compared to toluene.

Fluorescence quantum yields Φ_{Fl} were recorded in toluene as well as PhCN and versus *Coumarin 2* ($\Phi_{\text{Fl}}=0.77$ ^[22]) and *Rhodamine B* in EtOH ($\Phi_{\text{Fl}}=0.7$ ^[23]) as references for NDIs and PDIs, respectively (Table 1).

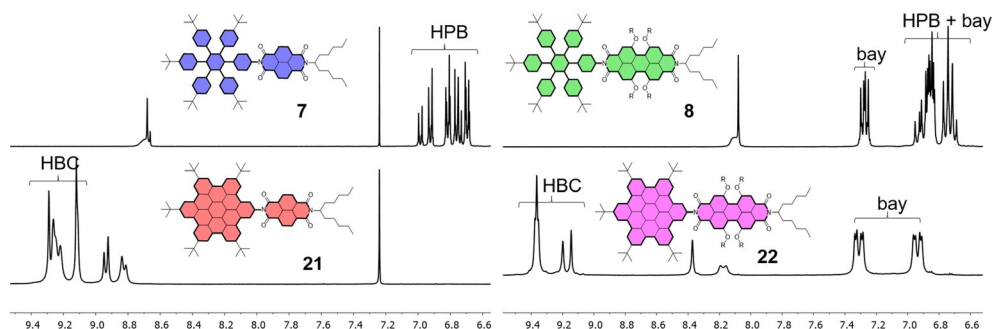


Figure 3. Aromatic region of $^1\text{H-NMR}$ spectra; left: NDI-HPB **7** (top) and NDI-HBC **21** (bottom); right: PDI-HPB **8** (top) and PDI-HBC **22** (bottom).

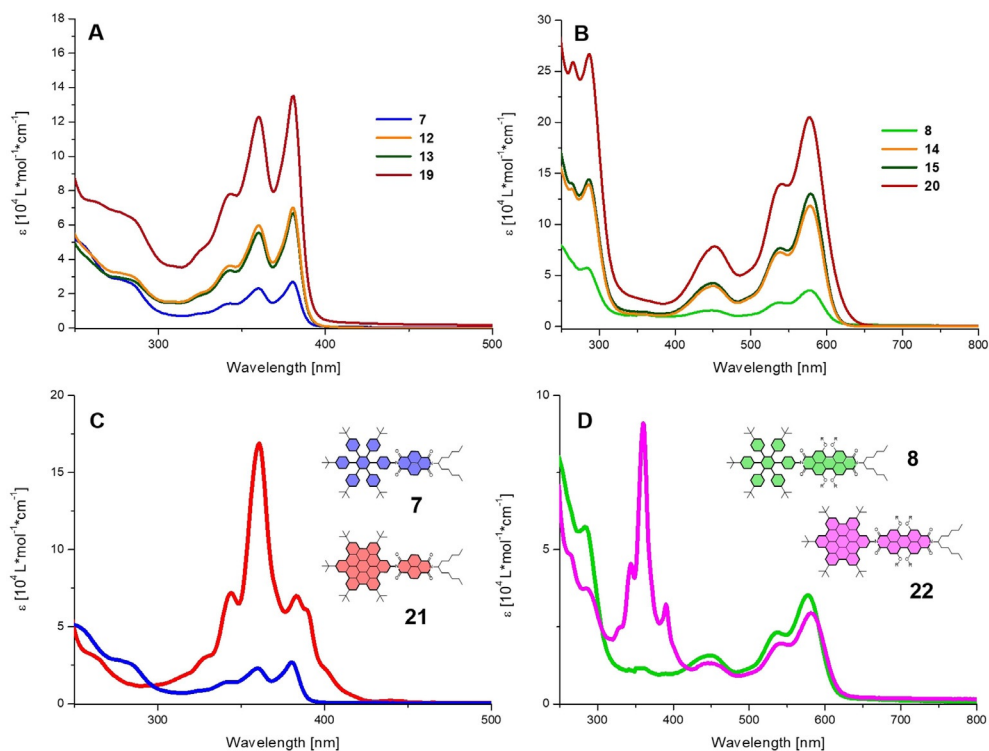


Figure 4. UV-vis absorption spectra of A) NDI-HPBs **7**, **12**, **13**, and **19** B) PDI-HPBs **8**, **14**, **15**, and **20** C) NDI-HPB **7** and NDI-HBC **21**. D) PDI-HPB **8** and PDI-HBC **22**.

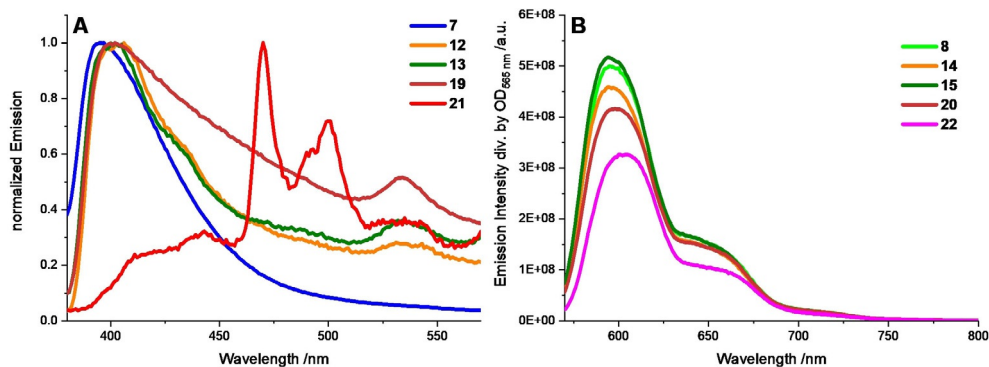


Figure 5. Steady-state fluorescence spectra of A) NDIs **7**, **12**, **13**, **19**, and **21** upon excitation at 300 nm in DCM (normalized) and B) PDIs **8**, **14**, **15**, **20**, and **22** upon excitation at 565 nm in toluene (intensity divided by OD at excitation) at room temperature.

Table 1. Fluorescence quantum yields of NDIs 7 , 12 , 13 , 19 , and 21 and PDIs 8 , 14 , 15 , 20 , and 22 in toluene and PhCN at room-temperature.					
NDIs	$\Phi_{\text{Fl, tol}}$	$\Phi_{\text{Fl, PhCN}}$	PDIs	$\Phi_{\text{Fl, tol}}$	$\Phi_{\text{Fl, PhCN}}$
7	< 0.001	–	8	0.83	0.75
12	< 0.001	–	14	0.76	0.53
13	< 0.001	–	15	0.84	0.74
19	0.001	0.002	20	0.69	0.33
21	< 0.001	–	22	0.60	0.012

All NDIs lack any appreciable fluorescence upon excitation at 365 nm with quantum yields of around or below 0.1% re-

gardless of the solvent polarity. PDI-HPBs all show strong fluorescence in both solvents, while yields tend to be lower in PhCN but still in the same order of magnitude. For PDI-HBC **22**, the fluorescence is quenching with yields of 60% and about 1% in toluene and PhCN, respectively.

Electrochemistry

Differential pulse and cyclic voltammetry were carried out in DCM with 0.1 M TBAPF₆ as electrolyte and a three electrode setup. Glassy carbon and a Pt-wire served as working electrode and counter electrode, respectively, while an Ag/AgCl reference electrode was used.

Table 2. Electrochemical redox potentials of **8**, **14**, **15**, **20**, and **22** vs. Fc^+/Fc (0.4 V vs. SHE) obtained by differential pulse voltammetry in 0.1 M TBAPF₆/DCM as electrolyte.

	E_{red}^2	E_{red}^1	E_{ox}^1	E_{ox}^2
PDI-HPB 8	−1.01	−0.84		+1.22
PDI-HBC 22	−0.93	−0.76	+1.13	+1.24
PDI ₃ -HPB-u 14	−1.00	−0.83		+1.23
PDI ₃ -HPB-s 15	−1.00	−0.83		+1.23
PDI ₆ -HPB 20	−0.96	−0.83		+1.24

The PDI compounds exhibit similar oxidations and reductions (Table 2). In PDI-HPB **8**, the first and second reductions appear at −0.84 and −1.01 V, respectively, and the oxidation at +1.22 V. In PDI₃-HPB-u **14** and PDI₃-HPB-s **15**, the reduction and oxidation potentials are both shifted by 0.01 V. In PDI₆-HPB **20**, the second reduction is further shifted to −0.96 V, while the first reduction remained at −0.83 V. The corresponding oxidation is observed at +1.23 V. In case of PDI-HBC **22**, the reductions are observed at −0.93 and −0.76 V. In addition to the oxidation at +1.24 V, PDI-HBC **22** possesses a further oxidation at +1.13 V. This oxidation is HBC-centred. Cyclic voltammetric measurements corroborate the reversibility of the oxidations and reductions (Figures S59, S61, S63, S65, S67).

All NDI compounds exhibit two reductions, which again down-shift with the numbers of attached NDIs and the change from HPB to HBC (Table 3). Except for NDI-HBC **21**, which features HBC-related oxidations at +1.04 and +1.19 V, all NDIs have oxidations above +1.7 V. However, DCM is electrochemically active at such potentials, which limits the accessible range to detect NDI-related oxidations. Therefore, we limit our discussion in the following to only the reductions. In NDI-HPB **7**, the reductions occur at −0.74 and −1.18 V. Moving on to the tri-substituted NDIs, no appreciable shifts are observed. A closer look at the intensity ratio between the first and second reductions in the monomer and the trimers reveals subtle changes. While the intensity ratio in the monomer was approximately 1:1, the second reduction is lower in intensity in the trimers. In the hexamer, this trend is even more pronounced. The second reduction, which is now seen at −1.10 V, is of comparatively low intensity and broad. In NDI-HBC **21**, the ratio is approximately 1:1 again. The reductions evolved at −0.65 and −1.11 V. By means of cyclic voltammetry, the reversibility of the reductions and oxidations were independently confirmed (Figures S53, S54, S55, S56, S57).

Table 3. Electrochemical redox potentials of **7**, **12**, **13**, **19**, and **21** vs. Fc^+/Fc (0.4 V vs. SHE) obtained by differential pulse voltammetry in 0.1 M TBAPF₆/DCM as electrolyte.

	E_{red}^2	E_{red}^1	E_{ox}^1	E_{ox}^2
NDI-HPB 7	−1.18	−0.74		
NDI-HBC 21	−1.11	−0.65	+1.04	+1.19
NDI ₃ -HPB-u 12	−1.18	−0.74		
NDI ₃ -HPB-s 13	−1.18	−0.74		
NDI ₆ -HPB 19	−1.10	−0.74		

Conclusion

We have presented the successful synthesis of NDI-HPBs as well as PDI-HPBs. Co-catalysed cyclotrimerization reactions were used, which allow controlling the tri- and hexa-substitution pattern on the HPBs. For the formation of mono-rylene HPBs, a simple imidization reaction was utilized. Investigation of Scholl oxidation showed that tri-substituted and hexa-substituted structures failed to close to the corresponding HBC derivatives, probably due to a decreased electron density on the HPB as a consequence of too many rylene-diimide units attached to it. Mono-substituted rylene-diimide-HBC were, however, successfully synthesized. In the case of PDI-HPB **8**, the Scholl oxidation needs to be performed at −78 °C to avoid undesirable side reactions, while reactions with the NDI derivative works out well at 0 °C without the formation of major side-products. All NDI conjugates exhibit very low fluorescence quantum yields. The quantum yields of the PDI conjugates are much higher and reveal a strong solvent polarity dependence, which is interesting for further excited state investigations. Since the synthesis of higher substituted rylene-diimide-HBCs via this synthetic route is not expedient, studies are in progress in our lab to find new synthetic strategies to complete the series of rylene-diimide-HBCs. Furthermore, generation of di-substituted HPBs and their toleration during Scholl oxidation are currently under investigation.

Experimental Section

Chemicals were purchased from Sigma–Aldrich and used without any further purification. Solvents were distilled prior to usage. Thin layer chromatography (TLC) was performed on Merck silica gel 60 F524, detected by UV-light (254 nm, 366 nm). Plug chromatography and column chromatography were performed on Macherey–Nagel silica gel 60 m (deactivated, 230–400 mesh, 0.04–0.063 mm). NMR spectra were recorded on a Bruker Avance 400 (¹H: 400 MHz, ¹³C: 101 MHz), a Bruker Avance 500 (¹H: 500 MHz, ¹³C: 126 MHz), or a Bruker Avance Neo Cryo-Probe DCH (¹H: 600 MHz, ¹³C: 150 MHz). Deuterated solvents were purchased from Sigma–Aldrich and used as received. Chemical shifts are given in ppm at room temperature and are referenced to residual protic impurities in the solvents (¹H: CHCl₃: 7.24 ppm; CH₂Cl₂: 5.32 ppm) or the deuterated solvent itself (¹³C{¹H}: CDCl₃: 77.16 ppm, CD₂Cl₂: 54.00 ppm). The resonance multiplicities are indicated as “s” (singlet), “brs” (broad singlet), “d” (doublet), “t” (triplet), “q” (quartet) and “m” (multiplet). Mass spectrometry was carried out with a Shimadzu AXIMA Confidence (MALDI-TOF, matrix: 2,5-dihydroxybenzoic acid DHB, *trans*-2-[3-(4-tert-butylphenyl)-2-methyl-2-propenylidene]malononitrile, DCTB) or without matrix (OM). High resolution mass spectrometry (HRMS) was recorded on a LDI/MALDI-ToF Bruker Ultraflex Extreme machine or on a APPI-ToF mass spectrometer Bruker maXis 4G UHR MS/MS spectrometer. IR spectra were recorded on a Bruker FT-IR Tensor 27 spectrometer with a Pike MIRacle ATR unit. UV/vis spectroscopy was carried out on a Varian Cary 5000 UV-vis-NIR spectrometer. The spectra were recorded at rt in DCM in quartz cuvettes (edge length = 1 cm) under ambient conditions. Fluorescence spectra were obtained from a Shimadzu RF-5301 PC and a NanoLog spectrofluorometer (Horiba Scientific).

General procedure for the synthesis of tolan precursors (GP I)

A dry flask was charged with rylene monoimide, amino-tolan and imidazole and the mixture was stirred under nitrogen at 120 °C until no starting material was left anymore. The crude was washed with H₂O and extracted with DCM. The combined organic layers were concentrated under reduced pressure and the mixture was purified by plug chromatography to provide the pure product.

General procedure for the cyclotrimerisation (GP II)

A 5 mL MW-vial was charged with rylene diimide-tolan, Co₂(CO)₈ and toluene (2.5 mL) and sealed with a septum. The reaction mixture was degassed with N₂ for 20 minutes and heated to 140 °C for 18 h. The solvent was removed under reduced pressure and the crude was purified by plug and silica gel chromatography to provide the pure products.

NDI-HPB (7)

Naphthalenemonimide **4** (37 mg, 86 μmol, 1.2 equiv), amino-HPB **6** (60 mg, 72 μmol, 1 equiv) and imidazole (500 mg) were stirred at 140 °C for 2 h. The reaction mixture was cooled to rt, dissolved in DCM and washed with H₂O. The crude product was subjected to plug chromatography (SiO₂, DCM) to provide the title compound as a beige solid (64 mg, 52 μmol, 72%). ¹H-NMR (CDCl₃, 400 MHz, 25 °C): δ = 0.78–0.82 (m, 6H, CH₃), 1.08–1.11 (m, 27H, CH₃), 1.15 (s, 18H, CH₃), 1.20–1.30 (m, 12H, CH₂), 1.78–1.87 (m, 2H, CH₂), 2.14–2.24 (m, 2H, CH₂), 5.10–5.17 (m, 1H, N-CH), 6.68–6.83 (m, 18H, Ar-CH), 6.90–6.94 (m, 4H, Ar-CH), 6.97–7.01 (m, 2H, Ar-CH), 8.66–8.74 (m, 4H, Ar-H) ppm; ¹³C-NMR (CDCl₃, 101 MHz, 25 °C): δ = 14.1 (CH₃), 22.7, 26.7 (CH₂), 31.35, 31.38 (CH₃), 31.8, 32.4 (CH₂), 34.2, 34.3 (C), 55.4 (CH), 123.2, 123.6, 126.6, 126.9, 127.07, 127.12, 131.1, 131.20, 131.23, 131.3, 131.6, 132.7, 137.7, 137.9, 138.0, 139.3, 140.4, 140.7, 141.1, 142.4, 147.7, 148.1 (Ar-CH, Ar-C), 162.8 (C=O) ppm; MS (MALDI-TOF, dctb): *m/z* = 1232.7758 (C₈₇H₉₆N₂O₄ [M]⁺); HRMS (MALDI-TOF, dctb): calculated for C₈₇H₉₆N₂O₄ ([M]⁺) *m/z* = 1232.7365, found *m/z* = 1232.7414; IR (ATR, rt): $\tilde{\nu}$ = 2957, 2926, 2861, 1708, 1667, 1580, 1512, 1451, 1326, 1248, 1191, 1099, 1018, 832, 769 cm⁻¹; UV/Vis (CH₂Cl₂): λ [nm] (ε [M⁻¹ cm⁻¹]) = 343 (14 000), 360 (23 000), 380 (27 000).

NDI-HBC (21)

NDI-HPB **7** (35 mg, 28 μmol, 1 equiv) was dissolved in DCM (5 mL) and cooled to 0 °C with an ice bath. After degassing with N₂ for 20 min a solution of dry FeCl₃ (74 mg, 0.45 mmol, 16 equiv) in MeNO₂ (0.25 mL) was added. The mixture was degassed for further 15 minutes and stirred overnight. The reaction was quenched via the addition of MeOH. The solvent was removed under reduced pressure and the crude product was purified by plug chromatography (SiO₂, DCM; THF:hexanes 1:9) to provide the title compound as a light yellow solid (29 mg, 24 μmol, 85%). ¹H-NMR (CDCl₃, 300 MHz, 25 °C): δ = 0.85–0.89 (m, 6H, CH₃), 1.24–1.36 (m, 12H, CH₂), 1.71 (s, 18H, CH₃), 1.79 (s, 18H, CH₃), 1.84 (s, 9H, CH₃), 1.89–2.00 (m, 2H, CH₂), 2.23–2.33 (m, 2H, CH₂), 5.17–5.28 (m, 1H, N-CH), 8.81–8.95 (m, 4H, Ar-CH), 9.10–9.30 (m, 12H, Ar-CH) ppm; ¹³C-NMR (CDCl₃, 101 MHz, 25 °C): δ = 14.0 (CH₃), 22.6, 26.7, 31.7 (CH₂), 31.94, 31.97, 32.04 (CH₃), 32.2 (CH₂), 35.69, 35.72, 35.75 (C), 55.4 (CH), 118.8, 118.9, 119.0, 119.5, 199.6, 119.9, 120.6, 120.9, 121.1, 121.5, 123.77, 123.79, 123.9, 126.2, 126.8, 127.2, 127.3, 129.6, 130.3, 130.4, 130.5, 130.6, 130.9, 131.6, 132.7, 133.3, 148.98, 149.0, 149.2 (Ar-CH, Ar-C), 163.9 (C=O) ppm; MS (MALDI-TOF, dctb): *m/z* = 1220.7211

(C₈₇H₈₄N₂O₄ [M]⁺); HRMS: (MALDI-TOF, dctb): calculated for C₈₇H₈₄N₂O₄ ([M]⁺) *m/z* = 1220.6426, found *m/z* = 1220.6395; IR (ATR, rt): $\tilde{\nu}$ = 2958, 2930, 2862, 1708, 1668, 1580, 1451, 1390, 1327, 1248, 1191, 1102, 1018, 833 cm⁻¹; UV/Vis (CH₂Cl₂): λ [nm] (ε [M⁻¹ cm⁻¹]) = 342 (31 000), 360 (48 000), 381 (57 000).

PDI-HPB (8)

Perylenemonimide **5** (50 mg, 44 μmol, 1.2 equiv), amino-HPB **6** (30 mg, 37 μmol, 1 equiv) and imidazole (500 mg) were stirred at 140 °C for 4 h. The reaction mixture was cooled to rt, dissolved in DCM and washed with H₂O. The crude product was subjected to plug chromatography (SiO₂, DCM) to provide the title compound as a pink solid (22 mg, 11 μmol, 31%). ¹H-NMR (CD₂Cl₂, 300 MHz, 25 °C): δ = 0.80–0.83 (m, 6H, CH₃), 1.08 (s, 18H, CH₃), 1.11 (s, 27H, CH₃), 1.20–1.24 (m, 12H, CH₂), 1.29–1.31 (m, 36H, CH₃), 1.68–1.78 (m, 2H, CH₂), 2.08–2.18 (m, 2H, CH₂), 5.01–5.11 (m, 1H, N-CH), 6.69–6.77 (m, 12H, Ar-CH), 6.83–6.95 (m, 20H, Ar-CH), 7.25–7.30 (m, 8H, Ar-CH) ppm; ¹³C-NMR (CD₂Cl₂, 101 MHz, 25 °C): δ = 14.3 (CH₃), 23.2, 27.0, 31.42, 31.44, 31.70, 31.73, 31.8, 32.3, 32.8 (CH₃, CH₂), 34.50, 34.54, 34.78, 34.80 (C), 55.0 (N-CH), 119.2, 119.7, 119.9, 120.3, 120.4, 120.6, 121.4, 123.4, 123.8, 124.1, 127.2, 127.28, 127.31, 131.6, 132.7, 133.1, 133.5, 133.7, 138.3, 138.6, 138.7, 140.1, 140.9, 141.2, 141.5, 142.1, 147.9, 148.0, 148.48, 148.49, 148.8, 153.8, 153.9, 156.4, 156.6 (Ar-CH, Ar-C), 163.5 (C=O) ppm; MS (MALDI-TOF, dctb): *m/z* = 1950.4522 (C₁₃₇H₁₄₈N₂O₈ [M]⁺); HRMS: (MALDI-TOF, dctb): calculated for C₁₃₇H₁₄₈N₂O₈ ([M]⁺) *m/z* = 1949.1230, found *m/z* = 1949.1264; UV/Vis (CH₂Cl₂): λ [nm] (ε [M⁻¹ cm⁻¹]) = 448 (16 000), 538 (23 000), 577 (35 000); Fluorescence (CH₂Cl₂): λ_{exc.} [nm] = 577, λ_{emission} [nm] (rel. int.) = 608 (100).

PDI-HBC (22)

PDI-HPB **8** (10 mg, 5.1 μmol, 1 equiv) was dissolved in DCM (20 mL) and cooled to –78 °C. After degassing with N₂ for 20 min a solution of dry FeCl₃ (13 mg, 82 μmol, 16 equiv) in MeNO₂ (0.1 mL) was added. The mixture was degassed for further 15 minutes and stirred overnight. The reaction was quenched via the addition of MeOH. The solvent was removed under reduced pressure and the crude product was purified by plug Chromatography (SiO₂, DCM:hexanes 1:1) to provide the title compound as a purple solid (5 mg, 2.6 μmol, 61%). ¹H-NMR (CD₂Cl₂, 600 MHz, 25 °C): δ = 0.83–0.85 (m, 6H, CH₃), 1.25–1.26 (m, 30H, CH₂, CH₃), 1.33 (s, 18H, CH₃), 1.76 (s, 18H, CH₃), 1.82–1.84 (m, 29H, CH₂, CH₃), 2.13–2.20 (m, 2H, CH₂), 5.06–5.14 (m, 1H, N-CH), 6.91–6.96 (m, 8H, Ar-CH), 7.29–7.34 (m, 8H, Ar-CH), 8.16–8.19 (m, 2H, Ar-CH), 8.37 (s, 2H, Ar-CH); 9.15 (s, 2H, Ar-CH), 9.20 (s, 2H, Ar-CH), 9.35–9.41 (m, 8H, Ar-CH) ppm; ¹³C-NMR (CD₂Cl₂, 150 MHz, 25 °C): δ = 14.4 (CH₃), 23.2, 27.1, 30.2, 31.7, 31.8, 32.25, 32.34, 32.9 (CH₃, CH₂), 34.8, 34.9, 36.25, 36.27, 36.28 (C), 55.1 (N-CH), 119.6, 119.8, 119.9, 120.0, 120.20, 120.24, 120.3, 120.6, 120.9, 121.16, 121.2, 121.4, 121.6, 122.1, 122.5, 123.4, 124.2, 124.3, 124.4, 126.3, 127.3, 130.3, 130.9, 130.96, 131.00, 131.1, 132.9, 133.5, 134.0, 135.3, 147.9, 148.0, 150.1, 150.2, 153.6, 153.9, 156.3, 156.8 (Ar-CH, Ar-C), 163.9, 164.7, 165.0 (C=O) ppm; MS (MALDI-TOF, dctb): *m/z* = 1938.1054 (C₁₃₇H₁₃₆N₂O₈ [M]⁺); HRMS: (MALDI-TOF, dctb): calculated for C₁₃₇H₁₃₆N₂O₈ ([M]⁺) *m/z* = 1937.0291, found *m/z* = 1937.0319; IR (ATR, rt): $\tilde{\nu}$ = 2955, 2955, 2859, 1698, 1661, 1585, 1504, 1409, 1339, 1210, 1173, 1111, 1014, 872, 834 cm⁻¹; UV/Vis (CH₂Cl₂): λ [nm] (ε [M⁻¹ cm⁻¹]) = 344 (45 500), 360 (91 000), 390 (32 000), 450 (13 000), 542 (20 000), 582 (29 500); Fluorescence (CH₂Cl₂): λ_{exc.} [nm] = 360, λ_{emission} [nm] (rel. int.) = 614 (100), λ_{exc.} [nm] = 582, λ_{emission} [nm] (rel. int.) = 614 (100).

NDI-tolane (10)

NDI-tolan **10** was prepared according to **GP I**: Naphthalenemonoimide **4** (85.0 mg, 0.20 mmol, 1 equiv), amino-tolan **9** (50.0 mg, 0.20 mmol, 1 equiv) and imidazole (1 g); plug chromatography (SiO₂, DCM); yield (beige solid) 49% (64.0 mg, 98.1 μmol). ¹H-NMR (CDCl₃, 400 MHz, 25 °C): δ = 0.79–0.83 (m, 6H, CH₃), 1.19–1.34 (m, 21H, CH₂, CH₃), 1.81–1.89 (m, 2H, CH₂), 2.16–2.25 (m, 2H, CH₂), 5.12–5.19 (m, 1H, N-CH), 7.27–7.29 (m, 2H, Ar-CH), 7.37–7.39 (m, 2H, Ar-CH), 7.47–7.49 (m, 2H, Ar-CH), 7.68–7.71 (m, 2H, Ar-CH), 8.71–8.80 (m, 4H, Ar-CH) ppm; ¹³C-NMR (CDCl₃, 101 MHz, 25 °C): δ = 14.2, 22.7, 26.7, 31.3, 31.8, 32.4, 34.9, (CH₃, CH₂), 55.5 (N-CH), 88.1, 90.9 (C≡C), 120.0, 124.9, 125.6, 126.5, 127.2, 128.7, 131.6, 132.8, 134.2, 152.0 (Ar-C, Ar-CH), 163.1 (C=O) ppm; MS (MALDI-TOF, dctb): *m/z* = 652.4360 (C₄₃H₄₄N₂O₄ [M]⁺); HRMS: (ESI, APPI): calculated for C₄₃H₄₄N₂O₄ ([M]⁺) *m/z* = 652.3296, found *m/z* = 652.3310; UV/Vis (CH₂Cl₂): λ [nm] (ε [M⁻¹ cm⁻¹]) = 343 (13 600), 360 (21 500), 381 (25 000).

PDI-tolane (11)

PDI-tolan **11** was prepared according to **GP I**: Perylenemonoimide **5** (114 mg, 0.100 mmol, 1 equiv), amino-tolan **9** (25.0 mg, 0.100 mmol, 1 equiv) and imidazole (1 g); plug chromatography (SiO₂, DCM); yield (pink solid) 50% (69.0 mg, 50.4 μmol). ¹H-NMR (CD₂Cl₂, 400 MHz, 25 °C): δ = 0.80–0.84 (m, 6H, CH₃), 1.19–1.24 (m, 12H, CH₂), 1.28 (s, 18H, CH₃), 1.31 (s, 18H, CH₃), 1.33 (s, 9H, CH₃), 1.72–1.79 (m, 2H, CH₂), 2.10–2.19 (m, 2H, CH₂), 5.04–5.11 (m, 1H, N-CH), 6.79–6.86 (m, 8H, Ar-CH), 7.23–7.29 (m, 10H, Ar-CH), 7.40–7.42 (m, 2H, Ar-CH), 7.48–7.50 (m, 2H, Ar-CH), 7.64–7.66 (m, 2H, Ar-CH), 8.06–8.09 (m, 2H, Ar-CH), 8.19 (s, 2H, Ar-CH) ppm; ¹³C-NMR (CD₂Cl₂, 101 MHz 25 °C): δ = 14.3 (CH₃), 23.1, 27.1, 31.4 (CH₂), 31.7, 32.2, 32.8 (CH₃, CH₂), 34.77, 34.81, 35.3 (C), 54.5 (N-CH), 88.5, 91.0 (C≡C), 119.6, 120.1, 120.2, 120.5, 120.6, 121.1, 122.0, 122.9, 124.5, 126.1, 127.3, 129.6, 131.9, 132.9, 133.5, 133.8, 135.9, 147.9, 148.1, 152.7, 153.5, 153.9, 156.2 (Ar-CH, Ar-C), 163.9 (C=O) ppm; MS (MALDI-TOF, dctb): *m/z* = 1369.8381 (C₉₃H₉₆N₂O₈ [M]⁺); HRMS: (ESI, APPI): calculated for C₉₃H₉₆N₂O₈ ([M]⁺) *m/z* = 1368.7161, found *m/z* = 1368.7203; UV/Vis (CH₂Cl₂): λ [nm] (ε [M⁻¹ cm⁻¹]) = 452 (6700), 541 (12 000), 581 (19 600); Fluorescence (CH₂Cl₂): λ_{exc.} [nm] = 541, λ_{emission} [nm] (rel. int.) = 612 (100).

Bis-NDI-tolane (17)

Bis-NDI-tolan **17** was prepared according to **GP I**: Naphthalenemonoimide **4** (0.20 g, 0.47 mmol, 2.2 equiv), di-amino-tolan **16** (45 mg, 0.22 mmol, 1 equiv) and imidazole (1 g); plug chromatography (SiO₂, DCM); yield (beige solid) 42% (93 mg, 92 μmol). ¹H-NMR (CDCl₃, 400 MHz, 25 °C): δ = 0.79–0.83 (m, 12H, CH₃), 1.19–1.33 (m, 24H, CH₂), 1.81–1.89 (m, 4H, CH₂), 2.15–2.26 (m, 4H, CH₂), 5.12–5.19 (m, 2H, N-CH), 7.31–7.33 (m, 4H, Ar-CH), 7.73–7.75 (m, 4H, Ar-CH), 8.74–8.81 (m, 8H, Ar-CH) ppm; ¹³C-NMR (CDCl₃, 101 MHz 25 °C): δ = 14.0 (CH₃), 22.5, 26.6, 31.6, 32.2 (CH₂), 55.3 (N-CH), 89.7 (C≡C), 124.1, 126.3, 127.0, 128.7, 130.8, 131.5, 132.8, 134.6 (Ar-C, Ar-CH), 162.9 (C=O) ppm; MS (MALDI-TOF, dctb): *m/z* = 1015.5605 (C₆₄H₆₂N₄O₈ [M]⁺); HRMS: (MALDI-TOF, dctb): calculated for C₆₄H₆₂N₄O₈ ([M]⁺) *m/z* = 1014.4562, found *m/z* = 1014.4583; UV/Vis (CH₂Cl₂): λ [nm] (ε [M⁻¹ cm⁻¹]) = 342 (31 000), 360 (48 000), 381 (57 000).

Bis-PDI-tolane (18)

Bis-PDI-tolan **18** was prepared according to **GP I**: Perylenemonoimide **5** (0.22 g, 0.19 mmol, 2.1 equiv), di-amino-tolan **16** (19 mg,

0.09 mmol, 1 equiv) and imidazole (500 mg); plug chromatography (SiO₂, DCM:hexanes 1:1 DCM); yield (pink solid) 27% (60 mg, 25 μmol). ¹H-NMR (CD₂Cl₂, 400 MHz, 25 °C): δ = 0.80–0.84 (m, 12H, CH₃), 1.18–1.26 (m, 24H, CH₂), 1.28 (s, 36H, CH₃), 1.31 (s, 36H, CH₃), 1.71–1.79 (m, 4H, CH₂), 2.09–2.20 (m, 4H, CH₂), 5.04–5.11 (m, 2H, N-CH), 6.80–6.86 (m, 16H, Ar-CH), 7.24–7.30 (m, 20H, Ar-CH), 7.67–7.69 (m, 4H, Ar-CH), 8.08 (brs, 4H, Ar-CH), 8.19 (s, 4H, Ar-CH) ppm; ¹³C-NMR (CD₂Cl₂, 101 MHz 25 °C): δ = 14.2, 22.9, 26.9, 31.6, 32.1, 32.7, 34.6, 34.7 (CH₃, CH₂), 54.9 (N-CH), 89.9 (C≡C), 119.3, 119.8, 119.9, 120.3, 120.8, 121.8, 122.6, 123.8, 126.99, 127.00, 129.4, 132.8, 133.2, 133.6, 136.0, 147.7, 147.9, 153.3, 153.6, 155.9, 156.6 (Ar-CH, Ar-C), 163.6 (C=O) ppm; MS (MALDI-TOF, dctb): *m/z* = 2448.6373 (C₁₆₄H₁₆₆N₄O₁₆ [M]⁺); HRMS: (MALDI-TOF, dctb): calculated for C₁₆₄H₁₆₇N₄O₁₆ ([M+H]⁺) *m/z* = 2448.2371, found *m/z* = 2448.2319; UV/Vis (CH₂Cl₂): λ [nm] (ε [M⁻¹ cm⁻¹]) = 452 (3000), 542 (5200), 583 (9000); Fluorescence (CH₂Cl₂): λ_{exc.} [nm] = 583, λ_{emission} [nm] (rel. int.) = 612 (100).

NDI₃-HPB (12) (13)

NDI₃-HPB **12** and **13** were prepared according to **GP II**: NDI-tolan **10** (90.0 mg, 0.138 mmol, 1 equiv), Co₂(CO)₈ (4.80 mg, 0.014 mmol, 0.1 equiv); plug chromatography (SiO₂, DCM + 5% acetone), silica gel chromatography (SiO₂, Hex:THF 9:1); yields: less symmetric NDI₃-HPB-u **12** (48.0 mg, 24.5 μmol, 53%); C3-symmetric NDI₃-HPB-s **13** (15.0 mg, 7.60 μmol, 17%).

NDI₃-HPB-u (12)

¹H-NMR (CDCl₃, 400 MHz, 25 °C): δ = 0.78–0.82 (m, 18H, CH₃), 1.17–1.32 (m, 63H, CH₃, CH₂), 1.78–1.89 (m, 6H, CH₂), 2.15–2.24 (m, 6H, CH₂), 5.10–5.18 (m, 3H, N-CH), 6.78–7.09 (m, 24H, Ar-CH), 8.64–8.76 (m, 4H, Ar-CH) ppm; ¹³C-NMR (CDCl₃, 101 MHz 25 °C): δ = 14.1 (CH₃), 22.6, 26.6 (CH₂), 31.3, 31.7, 32.3, 34.3, 34.4, 55.3 (CH), 123.8, 124.2, 126.8, 126.9, 127.12, 127.17, 127.5, 130.9, 131.2, 131.27, 131.33, 131.4, 131.6, 131.9, 132.1, 132.69, 132.73, 137.1, 137.32, 137.35, 139.6, 140.0, 140.3, 140.7, 141.0, 141.5, 141.69, 141.73, 142.1, 148.5, 148.9 (Ar-CH, Ar-C), 162.9, 163.2, 164.3 (C=O) ppm; MS (MALDI-TOF, dctb): *m/z* = 1958.9605 (C₁₂₉H₁₃₂N₆O₁₂ [M]⁺); HRMS: (ESI, APPI): calculated for C₁₂₉H₁₃₂N₆O₁₂ ([M]⁺) *m/z* = 1956.9898, found *m/z* = 1956.9885; IR (ATR, rt): $\tilde{\nu}$ = 2955, 2924, 2856, 1706, 1665, 1579, 1450, 1325, 1246, 1189, 1096, 1019, 767 cm⁻¹; UV/Vis (CH₂Cl₂): λ [nm] (ε [M⁻¹ cm⁻¹]) = 343 (36 000), 360 (60 000), 380 (70 000).

NDI₃-HPB-s (13)

¹H-NMR (CDCl₃, 300 MHz, 25 °C): δ = 0.80–0.82 (m, 18H, CH₃), 1.21–1.24 (m, 63H, CH₃, CH₂), 1.79–1.88 (m, 6H, CH₂), 2.14–2.24 (m, 6H, CH₂), 5.09–5.19 (m, 3H, N-CH), 6.78–6.88 (m, 12H, Ar-CH), 7.02–7.09 (m, 12H, Ar-CH), 8.68–8.78 (m, 4H, Ar-CH) ppm; ¹³C-NMR (CDCl₃, 101 MHz 25 °C): δ = 14.1 (CH₃), 22.6, 26.6 (CH₂), 31.3, 31.7, 32.3, 34.3 (CH₃, CH₂), 55.3 (N-CH), 118.7, 124.2, 126.8, 126.9, 127.1, 127.2, 131.2, 131.4, 131.9, 132.7, 137.1, 139.9, 141.1, 142.0, 148.9 (Ar-CH, Ar-C), 162.9 (C=O) ppm; MS (MALDI-TOF, dctb): *m/z* = 1958.4029 (C₁₂₉H₁₃₂N₆O₁₂ [M]⁺); HRMS: (MALDI-TOF, dctb): calculated for C₁₂₉H₁₃₂N₆O₁₂ ([M]⁺) *m/z* = 1979.9795, found *m/z* = 1979.9841; IR (ATR, rt): $\tilde{\nu}$ = 2957, 2922, 2856, 1706, 1665, 1579, 1450, 1325, 1249, 1190, 1096, 1019, 768 cm⁻¹; UV/Vis (CH₂Cl₂): λ [nm] (ε [M⁻¹ cm⁻¹]) = 343 (33 500), 360 (56 000), 381 (67 000).

PDI₃-HPB (14) (15)

PDI₃-HPB **14** and **15** were prepared according to **GP II**: PDI-tolan **11** (120 mg, 87.6 μmol, 1 equiv), Co₂(CO)₈ (2.99 mg, 9.00 μmol, 0.1 equiv); plug chromatography (SiO₂, DCM:hexanes 3:2), silica gel chromatography (SiO₂, DCM:hexanes 1:13:2); yields: less symmetric PDI₃-HPB-**u** **14** (79.0 mg, 19.1 μmol, 66%); C3-symmetric PDI₃-HPB-**s** **15** (21.0 mg, 5.08 μmol, 17%).

PDI₃-HPB-u (14)

¹H-NMR (CD₂Cl₂, 400 MHz, 25 °C): δ = 0.79–0.83 (m, 18H, CH₃), 1.01 (s, 9H, CH₃), 1.06 (s, 9H, CH₃), 1.08 (s, 9H, CH₃), 1.18–1.25 (m, 72H, CH₂, CH₃), 1.29–1.30 (m, 72H, CH₃), 1.69–1.77 (m, 6H, CH₂), 2.09–2.17 (m, 6H, CH₂), 5.02–5.09 (m, 3H, N-CH), 6.70–6.97 (m, 48H, Ar-CH), 7.18–7.29 (m, 24H, Ar-CH), 8.07–8.13 (m, 12H, Ar-CH) ppm.; ¹³C-NMR (CD₂Cl₂, 150 MHz, 25 °C): δ = 14.4, 14.5 (CH₃), 23.1, 23.3 (CH₂), 27.1, 31.43, 31.45, 31.46, 31.7, 31.8, 32.3, 32.5, 32.9, 34.58, 34.60, 34.63, 34.75, 34.82, 34.84 (CH₃, CH₂), 55.1 (N-CH), 119.6, 119.7, 119.9, 120.2, 120.3, 120.35, 120.39, 120.6, 120.7, 121.26, 121.30, 123.1, 123.37, 123.41, 123.9, 124.1, 124.4, 127.08, 127.13, 127.17, 127.19, 127.3, 127.5, 131.5, 131.6, 132.6, 132.7, 133.2, 133.3, 133.4, 133.7, 137.8, 138.06, 138.08, 139.9, 140.2, 140.8, 141.2, 141.40, 141.43, 141.45, 141.6, 141.8, 144.1, 145.6, 147.7, 147.8, 147.9, 148.7, 148.8, 149.0, 153.6, 153.8, 156.17, 156.24, 156.5 (Ar-CH, Ar-C), 163.38, 163.40, 163.9, 165.0 (C=O) ppm; MS (ESI): *m/z* = 4132.2105 (C₂₇₉H₂₈₈N₆NaO₂₄ [M+Na]⁺); HRMS: (ESI): calculated for C₂₇₉H₂₈₈N₆Na₂O₂₄ [M+2Na]²⁺. *m/z* = 2076.0642, found *m/z* = 2076.0608; IR (ATR, rt): $\tilde{\nu}$ = 2955, 2924, 2856, 1697, 1660, 1584, 1502, 1408, 1337, 1282, 1211, 1172, 1014, 880, 831 cm⁻¹; UV/Vis (CH₂Cl₂): λ [nm] (ε [M⁻¹ cm⁻¹]) = 450 (40000), 538 (73000), 578 (120000); Fluorescence (CH₂Cl₂): λ_{exc.} [nm] = 578, λ_{emission} [nm] (rel. int.) = 612 (100).

PDI₃-HPB-s (15)

¹H-NMR (CD₂Cl₂, 500 MHz, 25 °C): δ = 0.80–0.82 (m, 18H, CH₃), 1.05 (s, 27H, CH₃), 1.20–1.24 (m, 36H, CH₂), 1.29 (s, 54H, CH₃), 1.31 (s, 54H, CH₃), 1.70–1.77 (m, 6H, CH₂), 2.09–2.17 (m, 6H, CH₂), 5.03–5.10 (m, 3H, N-CH), 6.70–6.72 (m, 6H, Ar-CH), 6.78–6.80 (m, 6H, Ar-CH), 6.84–6.86 (m, 24H, Ar-CH), 6.93–6.95 (m, 12H, Ar-CH), 7.26–7.30 (m, 24H, Ar-CH), 8.08–8.13 (m, 12H, Ar-CH) ppm.; ¹³C-NMR (CD₂Cl₂, 125 MHz, 25 °C): δ = 14.4, 14.5 (CH₃), 23.1, 23.3 (CH₂), 27.1, 31.4, 31.8, 32.3, 32.5, 32.9, 34.6, 34.82, 34.84 (CH₃, CH₂), 55.1 (N-CH), 119.7, 119.9, 120.3, 120.4, 120.6, 120.7, 121.3, 123.2, 123.4, 123.9, 124.4, 127.1, 127.2, 127.3, 131.5, 132.6, 133.1, 133.4, 133.7, 137.7, 140.4, 141.3, 141.8, 147.8, 147.9, 149.1, 153.7, 153.8, 156.3, 156.5 (Ar-CH, Ar-C), 163.4, 163.9, 165.0 (C=O) ppm; MS (MALDI-TOF, dctb): *m/z* = 4110.2410 (C₂₇₉H₂₈₈N₆O₂₄ [M]⁺); HRMS: (MALDI-TOF, dctb): calculated for C₂₇₉H₂₈₈N₆O₂₄ [M]⁺. *m/z* = 4106.1495, found *m/z* = 4106.1523; IR (ATR, rt): $\tilde{\nu}$ = 2956, 2926, 2858, 1699, 1661, 1587, 1503, 1408, 1337, 1280, 1211, 1172, 1109, 1014, 878, 831 cm⁻¹; UV/Vis (CH₂Cl₂): λ [nm] (ε [M⁻¹ cm⁻¹]) = 450 (43000), 538 (76000), 579 (130000); Fluorescence (CH₂Cl₂): λ_{exc.} [nm] = 579, λ_{emission} [nm] (rel. int.) = 608 (100).

NDI₆-HPB (19)

NDI₆-HPB **19** was prepared according to **GP II**: Bis-NDI-tolan **17** (60 mg, 59 μmol, 1 equiv), Co₂(CO)₈ (15 mg, 44 μmol, 0.75 equiv), plug chromatography (SiO₂, DCM+1%MeOH); yield 61% (36 mg, 12 μmol). ¹H-NMR (CDCl₃, 300 MHz, 25 °C): δ = 0.79–0.84 (m, 36H, CH₃), 1.18–1.34 (m, 72H, CH₂), 1.80–1.87 (m, 12H, CH₂), 2.14–2.25 (m, 12H, CH₂), 5.09–5.19 (m, 6H, N-CH), 7.08 (d, *J* = 8.4 Hz, 12H, Ar-

CH), 7.21 (d, *J* = 8.4 Hz, 12H, Ar-CH), 8.63–8.76 (m, 24H, Ar-CH) ppm.; ¹³C-NMR (CDCl₃, 101 MHz, 25 °C): δ = 14.2 (CH₃), 22.7, 26.7, 31.8, 32.4 (CH₂), 55.4 (N-CH), 126.9, 127.07, 127.13, 127.5, 127.7, 130.8, 131.1, 131.5, 132.6, 132.7, 140.5, 140.7 (Ar-C, Ar-CH), 162.8, 163.0, 164.2 (C=O) ppm; MS (MALDI-TOF, dctb): *m/z* = 3045.3665 (C₁₉₂H₁₈₆N₁₂O₂₄ [M]⁺), 3068.3502 (C₁₉₂H₁₈₆N₁₂NaO₂₄ [M+Na]⁺), 3084.3500 (C₁₉₂H₁₈₆N₁₂O₂₄K [M+K]⁺); HRMS: (MALDI-TOF, dctb): calculated for C₁₉₂H₁₈₆N₁₂O₂₄ ([M]⁺) *m/z* = 3043.3697, found *m/z* = 3043.3723; IR (ATR, rt): $\tilde{\nu}$ = 2957, 2922, 2853, 1708, 1659, 1452, 1341, 1249, 1189, 1096, 1014, 800, 767, 730 cm⁻¹; UV/Vis (CH₂Cl₂): λ [nm] (ε [M⁻¹ cm⁻¹]) = 343 (78000), 360 (123000), 381 (135000).

PDI₆-HPB (20)

PDI₆-HPB **20** was prepared according to **GP II**: Bis-PDI-tolan **18** (50 mg, 20 μmol, 1 equiv), Co₂(CO)₈ (5.2 mg, 15 μmol, 0.75 equiv); plug chromatography (SiO₂, DCM:hexanes 3:2); yield 56% (27 mg, 3.7 μmol). ¹H-NMR (CD₂Cl₂, 400 MHz, 25 °C): δ = 0.79–0.83 (m, 36H, CH₃), 1.09 (s, 108H, CH₃), 1.19–1.30 (m, 180H, CH₂, CH₃), 1.69–1.80 (m, 12H, CH₂), 2.08–2.20 (m, 12H, CH₂), 5.02–5.10 (m, 6H, N-CH), 6.73–6.84 (m, 60H, Ar-CH), 6.98 (d, *J* = 8.6 Hz, 12H, Ar-CH), 7.08 (d, *J* = 8.7 Hz, 24H, Ar-CH), 7.23 (d, *J* = 8.7 Hz, 24H, Ar-CH), 8.0° (s, 12H, Ar-CH), 8.10 (brs, 12H, Ar-CH) ppm; ¹³C-NMR (CD₂Cl₂, 101 MHz, 25 °C): δ = 14.4, 23.1, 27.1, 31.6, 31.8, 32.3, 32.9, 34.6, 34.8 (CH₃, CH₂), 55.1 (N-CH), 119.6, 120.0, 120.1, 120.4, 120.7, 121.3, 123.4, 127.0, 127.1, 127.9, 133.0, 133.4, 133.5, 133.7, 140.9, 147.6, 147.9, 153.6, 153.8, 156.1, 156.6 (Ar-CH, Ar-C), 163.4 (C=O) ppm; MS (ESI): *m/z* = 3674.3940 (C₄₉₂H₄₉₈N₁₂O₄₈ [M]²⁺); HRMS: (ESI): calculated for C₄₉₂H₄₉₈N₁₂Na₂O₄₈ ([M+2Na]²⁺) *m/z* = 3693.8340, found *m/z* = 3693.8460; IR (ATR, rt): $\tilde{\nu}$ = 2955, 2925, 2854, 1698, 1661, 1585, 1503, 1408, 1337, 1281, 1210, 1171, 1014, 879, 832 cm⁻¹; UV/Vis (CH₂Cl₂): λ [nm] (ε [M⁻¹ cm⁻¹]) = 452 (78000), 540 (140000), 577 (200000); Fluorescence (CH₂Cl₂): λ_{exc.} [nm] = 577, λ_{emission} [nm] (rel. int.) = 608 (100).

Acknowledgements

The authors thank the Deutsche Forschungsgemeinschaft (DFG-SFB 953 "Synthetic Carbon Allotropes", and the Graduate School Molecular Science (GSMS) for financial support. Open access funding enabled and organized by Projekt DEAL.

Conflict of interest

The authors declare no conflict of interest.

Keywords: hexabenzocoronene • hexaphenylbenzene • naphthalene • perylene • rylenediimide

- [1] a) X. Zhan, A. Facchetti, S. Barlow, T. J. Marks, M. A. Ratner, M. R. Wasielewski, S. R. Marder, *Adv. Mater.* **2011**, *23*, 268–284; b) C. Li, H. Wonneberger, *Adv. Mater.* **2012**, *24*, 613–636; c) Z. Chen, M. G. Debije, T. Debaerdemaeker, P. Osswald, F. Würthner, *ChemPhysChem* **2004**, *5*, 137–140; d) F. Würthner, M. Stolte, *Chem. Commun.* **2011**, *47*, 5109–5115.
- [2] a) F. Würthner, *Chem. Commun.* **2004**, 1564–1579; b) T. Weil, T. Vosch, J. Hofkens, K. Peneva, K. Müllen, *Angew. Chem. Int. Ed.* **2010**, *49*, 9068–9093; *Angew. Chem.* **2010**, *122*, 9252–9278; c) S. V. Bhosale, C. H. Jani, S. J. Langford, *Chem. Soc. Rev.* **2008**, *37*, 331–342; d) C. Jung, B. K. Müller, D. C. Lamb, F. Nolde, K. Müllen, C. Bräuchle, *J. Am. Chem. Soc.* **2006**, *128*, 5283–5291; e) Y. Lin, X. Zhan, *Mater. Horiz.* **2014**, *1*, 470; f) X. Zhang, J. Yao, C. Zhan, *Sci. China Chem.* **2016**, *59*, 209–217.

- [3] a) S. Rajaram, R. Shivanna, S. K. Kandappa, K. S. Narayan, *J. Phys. Chem. Lett.* **2012**, *3*, 2405–2408; b) J.-M. Nunzi, *C. R. Physique* **2002**, *3*, 523–542; c) N. Liang, W. Jiang, J. Hou, Z. Wang, *Mater. Chem. Front.* **2017**, *1*, 1291–1303.
- [4] J. M. Mativetsky, M. Kastler, R. C. Savage, D. Gentilini, M. Palma, W. Pisula, K. Müllen, P. Samori, *Adv. Funct. Mater.* **2009**, *19*, 2486–2494.
- [5] a) G. Liu, T. Koch, Y. Li, N. L. Doltsinis, Z. Wang, *Angew. Chem. Int. Ed.* **2019**, *58*, 178–183; *Angew. Chem.* **2019**, *131*, 184–189; b) Y. Guo, Z. Ma, X. Niu, W. Zhang, M. Tao, Q. Guo, Z. Wang, A. Xia, *J. Am. Chem. Soc.* **2019**, *141*, 12789–12796; c) D. Meng, H. Fu, C. Xiao, X. Meng, T. Wilians, W. Ma, W. Wei, B. Fan, L. Huo, N. L. Doltsinis, Y. Li, Y. Sun, Z. Wang, *J. Am. Chem. Soc.* **2016**, *138*, 10184–10190; d) D. Meng, G. Liu, C. Xiao, Y. Shi, L. Zhang, L. Jiang, K. K. Baldridge, Y. Li, J. S. Siegel, Z. Wang, *J. Am. Chem. Soc.* **2019**, *141*, 5402–5408; e) Y. Duan, X. Xu, H. Yan, W. Wu, Z. Li, Q. Peng, *Adv. Mater.* **2017**, *29*, 1605115; f) Y. Lin, Y. Wang, J. Wang, J. Hou, Y. Li, D. Zhu, X. Zhan, *Adv. Mater.* **2014**, *26*, 5137–5142; g) Y. Liu, C. Mu, K. Jiang, J. Zhao, Y. Li, L. Zhang, Z. Li, J. Y. L. Lai, H. Hu, T. Ma, R. Hu, D. Yu, X. Huang, B. Z. Tang, H. Yan, *Adv. Mater.* **2015**, *27*, 1015–1020; h) M. Schubert, D. Dolfen, J. Frisch, S. Roland, R. Steyrlauthner, B. Stillner, Z. Chen, U. Scherf, N. Koch, A. Facchetti, D. Neher, *Adv. Energy Mater.* **2012**, *2*, 369–380; i) Q. Wu, D. Zhao, A. M. Schneider, W. Chen, L. Yu, *J. Am. Chem. Soc.* **2016**, *138*, 7248–7251; j) L. Yang, Y. Chen, S. Chen, T. Dong, W. Deng, L. Lv, S. Yang, H. Yan, H. Huang, *J. Power Sources* **2016**, *324*, 538–546; k) L. Yang, W. Gu, L. Lv, Y. Chen, Y. Yang, P. Ye, J. Wu, L. Hong, A. Peng, H. Huang, *Angew. Chem. Int. Ed.* **2018**, *57*, 1096–1102; *Angew. Chem.* **2018**, *130*, 1108–1114; l) J. Zhang, Y. Li, J. Huang, H. Hu, G. Zhang, T. Ma, P. C. Y. Chow, H. Ade, D. Pan, H. Yan, *J. Am. Chem. Soc.* **2017**, *139*, 16092–16095; m) N. Zhou, H. Lin, S. J. Lou, X. Yu, P. Guo, E. F. Manley, S. Loser, P. Hartnett, H. Huang, M. R. Wasielewski, L. X. Chen, R. P. H. Chang, A. Facchetti, T. J. Marks, *Adv. Energy Mater.* **2014**, *4*, 1300785.
- [6] a) J. Liu, S. Xie, S. Feng, M. Li, L. Wu, X. Xu, X. Chen, C. Li, Z. Bo, *J. Mater. Chem. C* **2018**, *6*, 9336–9340; b) S. Yu, Y. Chen, J. Wu, D. Xia, S. Hong, X. Wu, J. Yu, S. Zhang, A. Peng, H. Huang, *ACS Appl. Mater. Interfaces* **2018**, *10*, 28812–28818.
- [7] J. Wu, W. Pisula, K. Müllen, *Chem. Rev.* **2007**, *107*, 718–747.
- [8] a) D. Käfer, A. Bashir, X. Dou, G. Witte, K. Müllen, C. Wöll, *Adv. Mater.* **2010**, *22*, 384–388; b) J. Wu, M. D. Watson, N. Tchebotareva, Z. Wang, K. Müllen, *J. Org. Chem.* **2004**, *69*, 8194–8204.
- [9] a) L. F. Dössel, V. Kamm, I. A. Howard, F. Laquai, W. Pisula, X. Feng, C. Li, M. Takase, T. Kudernac, S. de Feyter, K. Müllen, *J. Am. Chem. Soc.* **2012**, *134*, 5876–5886; b) P. Samori, A. Fechtenkötter, E. Reuther, M. D. Watson, N. Severin, K. Müllen, J. P. Rabe, *Adv. Mater.* **2006**, *18*, 1317–1321; c) S. Wang, L. Dössel, A. Mavrinskiy, P. Gao, X. Feng, W. Pisula, K. Müllen, *Small* **2011**, *7*, 2841–2846; d) J. Wu, J. Qu, N. Tchebotareva, K. Müllen, *Tetrahedron Lett.* **2005**, *46*, 1565–1568; e) M. M. Martin, C. Dusold, A. Hirsch, N. Jux, *J. Porphyrins Phthalocyanines* **2020**, *24*, 268–277; f) A. Hirsch, C. Dusold, D. Sharapa, F. Hampel, *Chem. Eur. J.* **2020**, <https://doi.org/10.1002/chem.202003402>.
- [10] M. M. Martin, M. Dill, J. Langer, N. Jux, *J. Org. Chem.* **2019**, *84*, 1489–1499.
- [11] a) J. Xie, W. Chen, Z. Wang, K. C. W. Jie, M. Liu, Q. Zhang, *Chem. Asian J.* **2017**, *12*, 868–876; b) C. Xue, R. Sun, R. Annab, D. Abadi, S. Jin, *Tetrahedron Lett.* **2009**, *50*, 853–856.
- [12] a) K. Tambara, N. Ponnuswamy, G. Hennrich, G. D. Pantoş, *J. Org. Chem.* **2011**, *76*, 3338–3347; b) B. Narayan, K. K. Bejagam, S. Balasubramanian, S. J. George, *Angew. Chem. Int. Ed.* **2015**, *54*, 13053–13057; *Angew. Chem.* **2015**, *127*, 13245–13249; c) W. S. Horne, N. Ashkenasy, M. R. Ghadiri, *Chem. Eur. J.* **2005**, *11*, 1137–1144; d) A. Morandeira, J. Fortage, T. Edvinsson, L. Le Pleux, E. Blart, G. Boschloo, A. Hagfeldt, L. Hammarström, F. Odobel, *J. Phys. Chem. C* **2008**, *112*, 1721–1728; e) C. Lu, M. Fujitsuka, A. Sugimoto, T. Majima, *J. Phys. Chem. C* **2016**, *120*, 12734–12741.
- [13] J. Fortage, M. Séverac, C. Houarner-Rassin, Y. Pellegrin, E. Blart, F. Odobel, *J. Photochem. Photobiol. A* **2008**, *197*, 156–169.
- [14] a) F. Würthner, A. Sautter, J. Schilling, *J. Org. Chem.* **2002**, *67*, 3037–3044; b) C. Huang, S. Barlow, S. R. Marder, *J. Org. Chem.* **2011**, *76*, 2386–2407.
- [15] R. Stężycki, D. Reger, H. Hoelzel, N. Jux, D. Gryko, *Synlett* **2018**, *29*, 2529–2534.
- [16] H. He, Y.-J. Wu, *Tetrahedron Lett.* **2004**, *45*, 3237–3239.
- [17] a) S. Kotha, E. Brahmachary, K. Lahiri, *Eur. J. Org. Chem.* **2005**, 4741–4767; b) N. E. Schore, *Chem. Rev.* **1988**, *88*, 1081–1119.
- [18] D. Nishimura, Y. Takashima, H. Aoki, T. Takahashi, H. Yamaguchi, S. Ito, A. Harada, *Angew. Chem. Int. Ed.* **2008**, *47*, 6077–6079; *Angew. Chem.* **2008**, *120*, 6166–6168.
- [19] a) L. Zhai, R. Shukla, S. H. Wadumethrige, R. Rathore, *J. Org. Chem.* **2010**, *75*, 4748–4760; b) M. Grzybowski, K. Skonieczny, H. Butenschön, D. T. Gryko, *Angew. Chem. Int. Ed.* **2013**, *52*, 9900–9930; *Angew. Chem.* **2013**, *125*, 10084–10115.
- [20] B. T. King, J. Kroulík, C. R. Robertson, P. Rempala, C. L. Hilton, J. D. Korišek, L. M. Gortari, *J. Org. Chem.* **2007**, *72*, 2279–2288.
- [21] M. M. Martin, D. Lungerich, F. Hampel, J. Langer, T. K. Ronson, N. Jux, *Chem. Eur. J.* **2019**, *25*, 15083–15090.
- [22] G. Gauglitz, A. Lorch, D. Oelkrug, *Z. Naturforsch. A* **1982**, *37*, 219–223.
- [23] F. L. Arbeloa, P. R. Ojeda, I. L. Arbeloa, *J. Lumin.* **1989**, *44*, 105–112.

Manuscript received: September 21, 2020

Revised manuscript received: October 30, 2020

Accepted manuscript online: November 3, 2020

Version of record online: December 28, 2020